EFFECT OF ZnS AS AN IMPURITY ON THE PHYSICAL PROPERTIES OF (NH_4) H_2PO_4 SINGLE CRYSTALS

J. Anitha Hudson[1], C.K. Mahadevan[2] , C.M. Padma[3]

[1,3]*Department of Physics, Women's Christian College, Nagercoil - 629 001, Tamil Nadu, India*
[2]*Physics Research Centre, S.T. Hindu College, Nagercoil - 629 002, Tamil Nadu, India*
anitha.hudson@gmail.com, mahadevan58@yahoo.co.in, padmajeyaraj@gmail.com

Abstract

Pure and ZnS added ADP (ammonium dihydrogen phosphate) single crystals have been grown at room temperature by the free evaporation method. A total of six crystals have been grown and characterized structurally, chemically, thermally, optically, mechanically and electrically by using the suitable standard methods. Results obtained indicate that the impurity molecules have entered into the ADP crystal matrix. ZnS addition is found to increase the SHG efficiency significantly. All the grown crystals exhibit good optical transmission in the entire visible region. Results of AC and DC electrical measurements indicate a normal dielectric behaviour for all the six crystals grown. The electrical parameters, viz., DC electrical conductivity, dielectric constant, dielectric loss factor and AC electrical conductivity are found to increase with the increase in temperature. The optical, mechanical and electrical parameters are found to vary nonlinearly with the impurity (ZnS) concentration.

Keywords: *ADP crystal, Crystal growth, Doped crystals, Physical properties, X-ray diffraction.*

----------***----------

1. INTRODUCTION

Ammonium dihydrogen phosphate (ADP, $NH_4H_2PO_4$) has superior physical properties and has been exploited for a variety of applications. ADP crystal is a representative of hydrogen-bonded crystals. It possesses antiferro-eletric, piezo-electric, electro-optic, dielectric and nonlinear optical properties. Applications of integrated electro-optics include high speed modulation and switching of optical signals for telecommunication and signal processing [1-6]. ADP crystal is antiferro-electric and belongs to orthorhombic crystal system with space group $P2_12_12_1$ below the temperature 148.5K. Above this temperature, it is para-electric and belongs to tetragonal crystal system with space group $I\bar{4}2d$ [7-9].

Several researchers have carried out a lot of studies on pure and doped (with organic and inorganic) ADP crystals. They have found that several physical properties of ADP crystals can be modified by adding impurities like Ni^{3+}, Mg^{2+}, ammonium malate, thiourea, L-lysine monohydrochloride dihydrate, L-alanine, L-arginine and ammonium acetate [10-22]. Currently, a special attention is being paid to modifying materials with nanostructured substances. Extensive research work has been carried out on the growth and characterization of KDP (potassium dihydrogen phosphate) doped with metal oxide nanoparticles like TiO_2 [23-29], CdTe nanoparticle [30] and organic dye molecules [31]. Several studies have been done on the preparation and properties of glass matrix embedded with semiconductor nanocrystals [32-34] and alkali halides crystals (KBr, NaCl, KCl, etc) doped with II-VI compounds (CdS, CdTe, etc) [35-37]. The density and mechanical properties of triglycine sulphate (TGS) crystals have been found to be improved by doping with water-soluble CdS nanoparticle dispersed in water [38].

The II-VI compound ZnS is an interesting material on account of its proven and potential applications in photoluminescent and electro-luminescent devices and also as an n-type window layer in heterojunction solar cells because of its large band gap 3.65 eV [39]. It is a promising material for opto-electronic device applications such as blue light emitting diode [40] and photovoltaic cells [41]. It will be interesting if we are able to dope ADP single crystals with ZnS. ADP single crystals are normally grown at near ambient temperatures by using the solution methods. But, generally, II-VI compounds including ZnS do not dissolve in water. Now, the challenging problem is to find a way to dissolve ZnS in the aqueous solution of ADP used for the growth of single crystals. The present study is an attempt in this direction.

There are few reports available which describe the preparation of water soluble CdS nanoparticles with complex molecules used as stabilizers and capping agents [42,43]. Tang et al [44] have prepared water-soluble CdS nanoparticles by surface modification with ethylene diamine. The ethylene diamine capped CdS nanoparticles are found to be slightly soluble in water.

In the present study, we have made an attempt to introduce ZnS as dopant into the ADP crystal matrix. Ethylene diamine capped ZnS nanoparticles were prepared by a simple solvothermal method using a domestic microwave oven (Mahadevan's method [45-47]). Pure and ZnS doped ADP single crystals (a total of six) were grown and characterized

chemically, structurally, thermally, optically, mechanically and electrically by using the suitable standard methods. We herein report the results obtained and discussed.

2. EXPERIMENTAL DETAILS

2.1 Preparation of ZnS nanoparticles

Ethylene diamine capped ZnS nanoparticles were prepared from zinc acetate dihydrate and thiourea (both AR grade) dissolved in double distilled water in the presence of ethylene diamine. Mahadevan's method [45-47] was adopted for the above purpose. The solubility was found to be 0.71g/100ml of H_2O. Details on the preparation and characterization of ZnS nanoparticles appear elsewhere.

2.2. Growth of ADP single crystals

Pure and ZnS doped ADP single crystals were grown from saturated aqueous solutions of ADP by using the slow (free) evaporation method. 0.1g ZnS nanoparticles were dissolved in 100ml double distilled water and used as the dopant. Five different dopant concentrations were considered by adding 1,2,3,4 and 5ml of the above solution to the ADP solution. The above doped solutions were stirred well and then allowed to equilibrate at room temperature in a dust free zone. In the beginning stage, small crystals appeared due to slow evaporation. They then grew larger in a considerable finite time. We represent the grown crystals in the same order as Pure ADP, ZADP-1, ZADP-2, ZADP-3, ZADP-4 and ZADP-5.

2.3. Characterizations made

An automated X-ray powder diffractometer (X-PERT PRO PANalytical) with monochromated CuK_α radiation (λ = 1.54056 Å) was used to collect the X-ray powder diffraction data in the 2θ range 10-70^0 for all the six powdered crystal samples. Procedures given by Lipson and Steeple [48] were followed to index all the reflection peaks. The lattice parameters were determined from the indexed data. The estimated standard deviations (e.s.d.s) were also determined. Fourier transform infrared (FTIR) spectra for the Pure ADP and ZADP-5 crystals were recorded by the KBr pellet method using a Perkin-Elmer FTIR spectrometer in the wavenumber range 400-4000cm^{-1}. Atomic absorption spectral (AAS) analysis was carried out for the doped crystals using an AAS spectrometer (Model AA-6300).

For the Pure ADP and ZADP-5 crystals, thermogravimetric analysis (TGA) and differential thermal analysis (DTA) were carried out using a thermal analyser (model SDT-Q600) in the nitrogen atmosphere in the temperature range of room temperature to 900^{0}C at a heating rate of 10^{0}C/min.

UV-Vis-NIR transmission spectra for all the six crystals grown were recorded using a Perkin-Elmer Lambda 35 spectrophotometer in the wavelength range 190-1100nm. All the six crystals grown were subjected to second harmonic generation (SHG) test by the Kurtz and Perry [49] powder method using a Q-switched Nd:YAG laser (λ=1064nm) supplied by Spectra physics, USA. The mechanical property of all the six grown crystals were understood by carrying out the Vickers microhardness measurements on the (100) face using a SHIMADZU HMV-2T microhardness tester with a diamond indentor.

AC and DC electrical measurements were carried out on all the six crystals along both a- and c- directions in the temperature range 40-150^{0}C. Crystals with large surface defect-free (i.e. without any pit or crack or scratch on the surface, tested with a traveling microscope) size (>3mm) were selected and used for the measurements. The extended portions of the crystals were removed completely and the opposite faces were polished and coated with good quality graphite to obtain a good conductive surface layer. The dimensions of the crystals were measured using a traveling microscope (Least count = 0.001cm). The observations were made while cooling the sample crystal and the temperature was controlled to an accuracy of $\pm$1^{0}C.

The DC electrical conductivity measurements were carried out to an accuracy of $\pm$2% by the conventional two-probe method using a million megohm meter in a way similar to that followed by Mahadevan and his co-workers [50,51]. The DC conductivity (σ_{dc}) of the crystal was calculated using the relations:

$$\sigma_{dc} = d_{crys}/(RA_{crys}) \quad (1)$$

where R is the measured resistance, d_{crys} is the thickness of the sample crystal and A_{crys} is the area of the face of the crystal in contact with the electrode.

The capacitance (C_{crys}) and dielectric loss factor ($\tan\delta$) measurements were carried out to an accuracy of $\pm$2% by the parallel plate capacitor method using an LCR meter (Systronics make) with a fixed frequency of 1 kHz in a way similar to that followed by Mahadevan and his co-workers [52,53]. The air capacitance (C_{air}) was also measured but only at 40^{0}C since the temperature variation of C_{air} was found to be negligible. As the crystal surface area touching the electrode was smaller than the plate (electrode) area of the cell, the dielectric constant of the crystal (ε_r) was calculated using Mahadevan's formula [54,55].

$$\varepsilon_r = \left[\frac{A_{air}}{A_{crys}}\right]\left[\frac{C_{crys}-C_{air}[1-A_{crys}/A_{air}]}{C_{air}}\right] \quad (2)$$

where C_{crys} is the capacitance with crystal (including air), C_{air} is the capacitance of air and A_{air} is the area of the electrode. The AC electrical conductivity (σ_{ac}) was calculated using the relation:

$$\sigma_{ac} = \varepsilon_0 \varepsilon_r \omega \tan\delta \quad (3)$$

where ε_0 is the permittivity of free space and ω is the angular frequency of the applied field.

The σ_{dc} and σ_{ac}values obtained could be fitted to the corresponding Arrhenius relation:

$$\sigma_{dc} = \sigma_{0dc}\exp[-E_{dc}/(kT)] \quad (4)$$

$$\sigma_{ac} = \sigma_{0ac}\exp[-E_{ac}/(kT)] \quad (5)$$

where σ_{0dc} and σ_{0ac} are the proportionality constants (considered to be characteristic constants of the material), k is the Boltzmann constant and T is the absolute temperature. The activation energies (E_{dc} and E_{ac}) were estimated from the slopes of the corresponding line plots between $ln\,\sigma_{dc}$ or $ln\sigma_{ac}$ and $10^3/T$.

3. RESULTS AND DISCUSSION

3.1 Crystals grown, lattice parameters and chemical composition

A photograph of the sample crystals grown in the present study is shown in Figure 1. All the six crystals grown are colourless, transparent and are stable in atmospheric air. The TGA and DTA curves obtained for pure ADP and ZADP-5 are shown in Figure 2 [(a) and (b)]. It can be understood that Pure ADP and ZADP-5 are thermally stable at least up to 180^0C and 174^0C respectively. The decomposition takes place at (about) these temperatures. The difference in thermal stability observed between these two crystals makes us to understand that ZnS molecules have entered into the ADP crystal matrix in the case of doped crystals.

Fig-1: Photograph showing the sample crystals grown in the present study

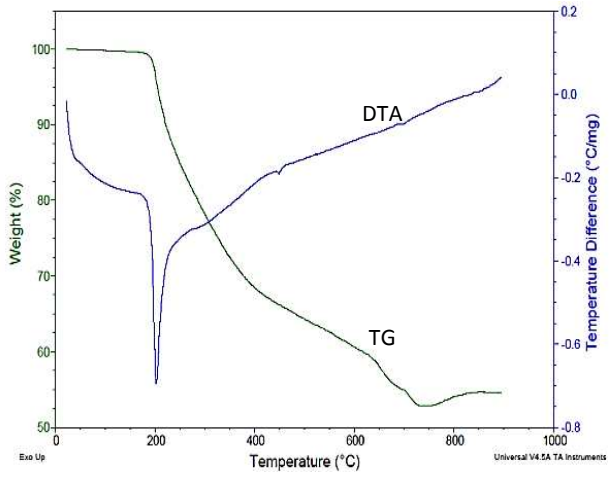

Fig-2 (a): TGA and DTA Curves observed for the Pure ADP

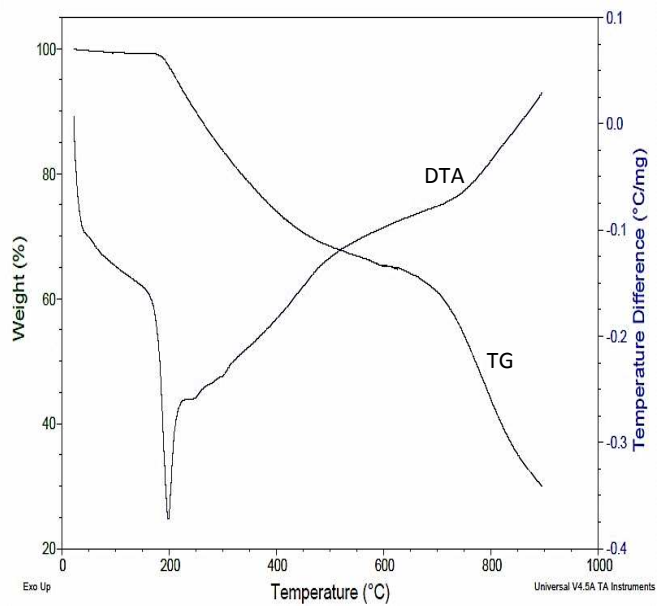

Fig-2 (b): TGA and DTA Curves observed for the ZADP-5

Figure 3 shows the indexed X-ray powder diffraction (PXRD) patterns observed in the present study. Appearance of sharp and strong peaks confirms the crystalline nature of all the six crystals grown. The average lattice parameters estimated through PXRD analysis and the Zn atom contents of doped crystals obtained through AAS analysis are given in Table 1.

Table-1: The observed average lattice parameters and Zn atom contents. The e.s.d.s. are given in parentheses.

Crystal	Lattice Parameters			Zn atom content (ppm)
	a (Å)	c (Å)	Volume (Å^3)	
PureADP	7.490 (1)	7.549 (6)	423.5	--
ZADP-1	7.482 (4)	7.581 (1)	424.4	0.20
ZADP-2	7.535 (1)	7.608 (2)	432.0	0.52
ZADP-3	7.562 (1)	7.655 (1)	437.7	0.67
ZADP-4	7.576 (4)	7.660 (1)	439.7	0.70
ZADP-5	7.601 (1)	7.730 (3)	446.6	0.82

The observed increase of lattice (unit cell) volume due to impurity addition (see Table 1) indicates that the impurity (ZnS) molecules have entered into the ADP crystal matrix. Further, it can be seen that the lattice volume increases with the increase in impurity concentration. The Zn atom contents observed through AAS analysis (see Table 1) endorse this result. The lattice parameters observed in the present study for the pure ADP crystal agree well with that reported in the literature [56]. a = 7.502 Å, c = 7.554 Å and volume = 425.1Å^3.This confirms the identity of the material (ADP) crystallized.

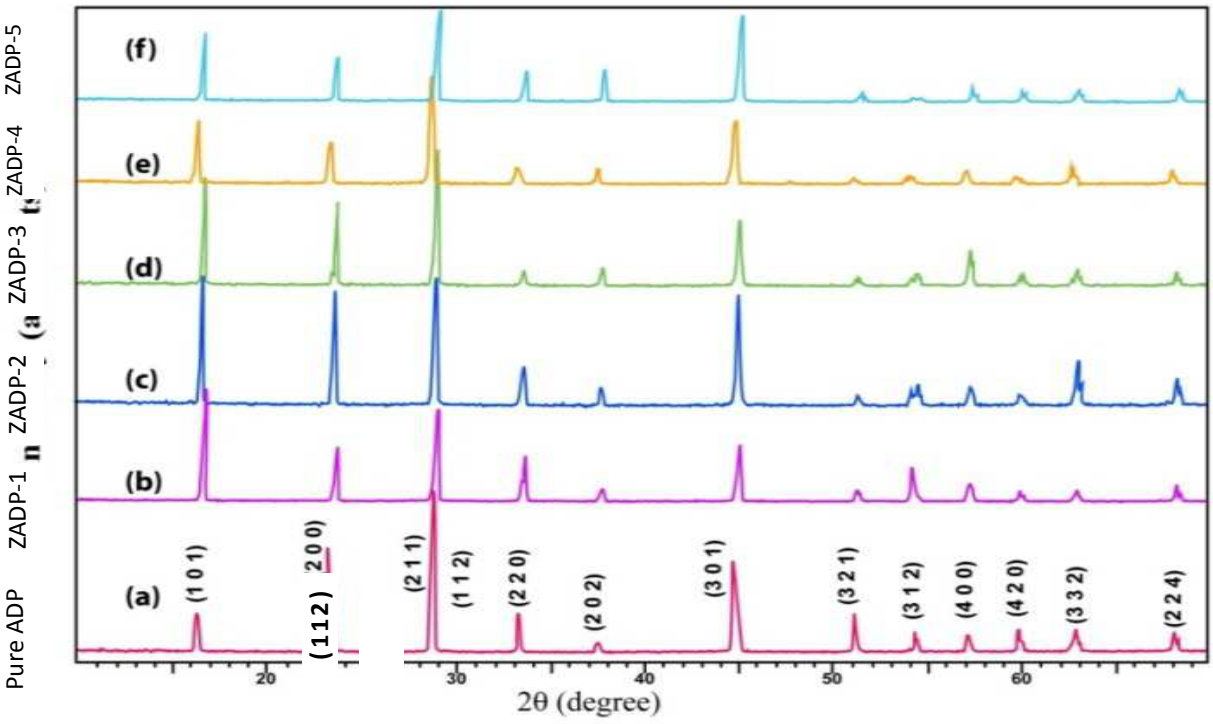

Fig-3: PXRD patterns observed for Pure and ZnS doped ADP crystals

The FTIR spectra observed in the present study for pure ADP and ZADP-5 are shown in Figure 4. The vibrational bands assigned are given in Table-2. The spectra indicate no significant difference due to doping as the dopant concentrations considered in the present study are small. Further, the spectrum observed for the pure ADP compares well with that reported in the literature [57]. The vibrational band assignments reported in the literature for pure ADP are also given in Table 2 for comparison. Further, the FTIR spectra observed also endorse the results obtained in the PXRD analysis in confirming the material of the substance crystallized.

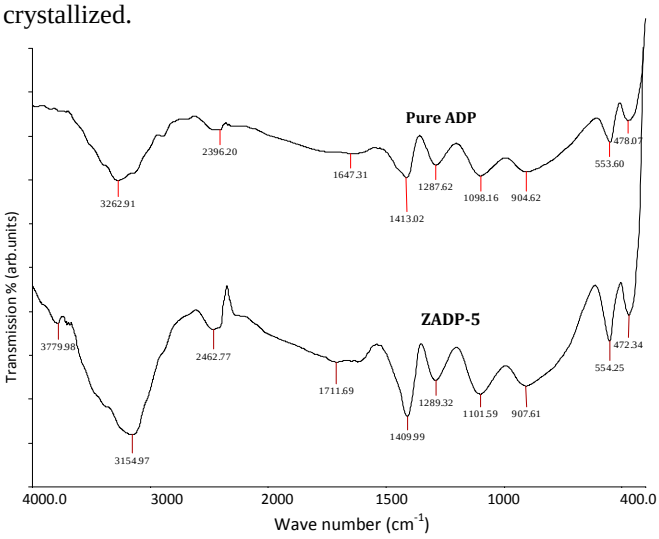

Fig-4: FTIR spectra observed for the Pure ADP and ZADP-5 crystals

Table-2: The vibrational band assignments

Wavenumbers (cm^{-1}) for			Assignment
Pure ADP (present)	ZADP-5	Pure ADP [57]	
3262	3154	3140	O-H Stretching
2396	2462	2370	Combination band of stretching
1647	1711	1646	N-H bonding of NH_4
1413	1409	1402	Bending stretching of NH_4
1287	1289	1293	Combination band of stretching
1098	1101	1090	P-O-H stretching
904	907	930	P-O-H stretching
553	554	544	PO_4 stretching
478	472	470	PO_4 stretching

3.2 Optical and mechanical properties

The UV-Vis-NIR spectra observed in the present study for all the six crystals grown are shown in Figure 5. The observed optical transmission percentages and cut off wavelengths are given in Table 3. The UV-Vis-NIR spectra indicate that both pure and ZnS doped ADP crystals exhibit good transmittances towards the visible and infrared regions and low cut off wavelengths. The observed transparent nature of these crystals is a desirable property for the grown crystals to have NLO applications.

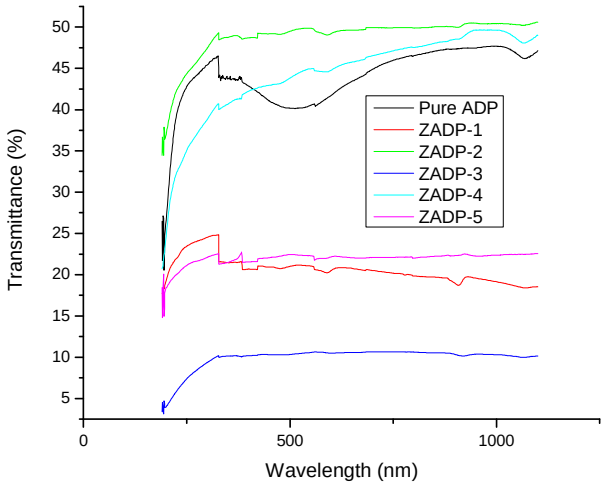

Fig-5: UV-Vis-NIR spectra observed for the Pure and ZnS doped ADP crystals

The second harmonic generation (SHG) efficiencies observed are provided in Table 3. It is found that the SHG efficiency increases significantly due to ZnS doping. In effect, the results obtained indicate that all the six crystals grown in the present study are NLO active.

Table-3: The cut off wave lengths, optical transmission percentages, SHG efficiencies and work hardening coefficients (n)

Crystals	Cutoff wave length (nm)	Optical transmission (%)	SHG efficiency (in ADP unit)	Work hardening co-efficient
Pure ADP	331	46	1.00	3.25
ZADP-1	328	22	4.68	3.82
ZADP-2	320	49	1.79	2.46
ZADP-3	313	10.5	1.14	3.75
ZADP-4	305	50	4.84	3.02
ZADP-5	300	22	3.75	2.92

The Vicker's hardness number (H_v) is defined as:

$$H_v = 1.8544\ P/d^2\ \ kg/mm^2 \qquad (6)$$

where P is the load applied and d is the diagonal length of the indentation made on the crystal surface. The Meyers law [58] is expressed as:

$$P = k_1 d^n \qquad (7)$$

where k_1 is the material constant and n is the Meyer index or work hardening co-efficient. Figure 6 shows the hardness behaviour (a) and log P versus log d plots (b). The work hardening co-efficients were estimated from the slopes of the best-fitted straight lines of log P versus log d curves.

The hardness of a material is a measure of its resistance it offers to local deformation and micro-indentation test is a useful method for understanding the nature of plastic flow and its influence on the deformation of the materials [59].

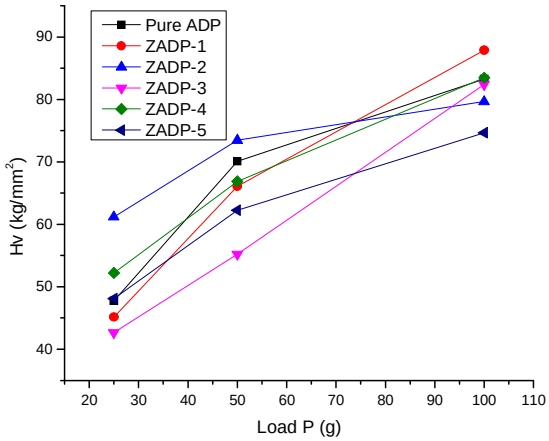

Fig-6 (a): Microhardness vs Load graph for Pure and ZnS doped crystals

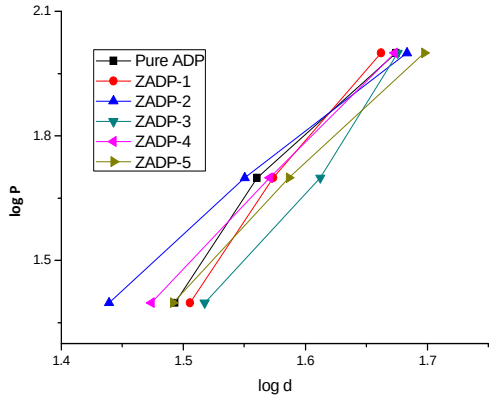

Fig-6 (b): log P vs log d graph for Pure and ZnS doped crystals

Also, higher hardness value of a crystal indicates that greater stress is required to create dislocation [60]. Results obtained in the present study indicate that the H_v value increases with the increasing load. Also, it increases up to a load of 100g, above which cracks start developing which may be due to the release of internal stress generation with indentation. According to Onitsch and Hanneman 'n' should have the value within 1.0 and 1.6 for hard materials and above 1.6 for soft ones [59]. The 'n' values observed in the present study are more than 1.6 indicating that all the six crystals grown belong to soft materials category.

3.3 Electrical properties

Figures 7-10 show the electrical parameters observed in the present study, viz. DC electrical conductivity (σ_{dc}), dielectric constant (ε_r), dielectric loss factor (tan δ) and AC electrical conductivity (σ_{ac}). All the four electrical parameters are found to increase with the increase in temperature. However, there is no systematic variation observed with the impurity concentration (volume of ZnS solution added to the ADP solution used for the growth of single crystals) for all the above four electrical parameters in the whole temperature range considered in the present study. Figures 11-14 illustrate this. Moreover, the ε_r values along both a- and c-

directions and σ_{dc} values along a-direction observed for the ZnS doped crystals are more than that observed for the pure ADP. But, the variation with ZnS concentration is nonlinear.

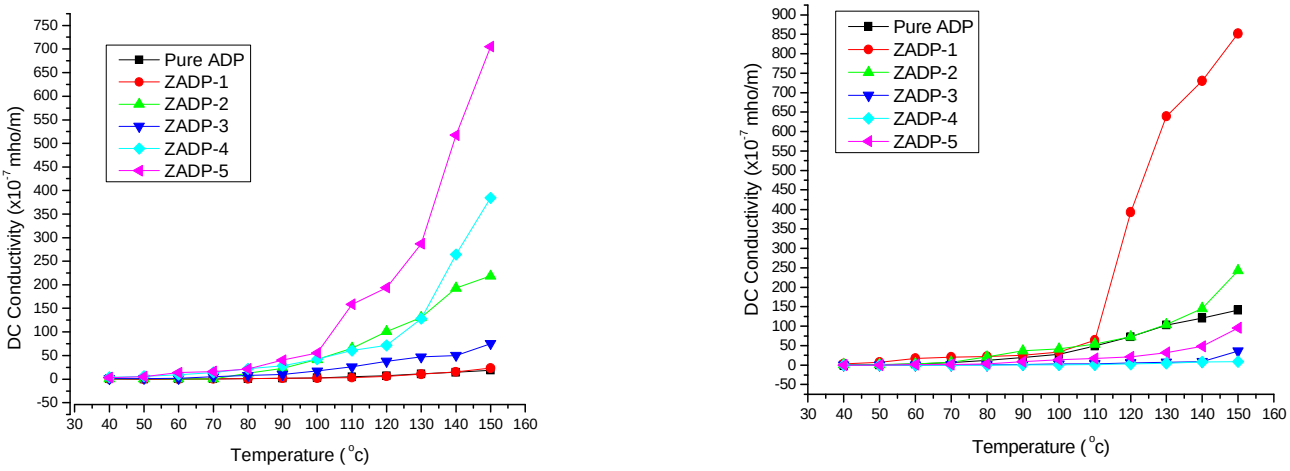

Along a-direction Along c-direction

Fig.7: DC electrical conductivities (σ_{dc}) observed for the Pure and ZnS doped ADP crystals

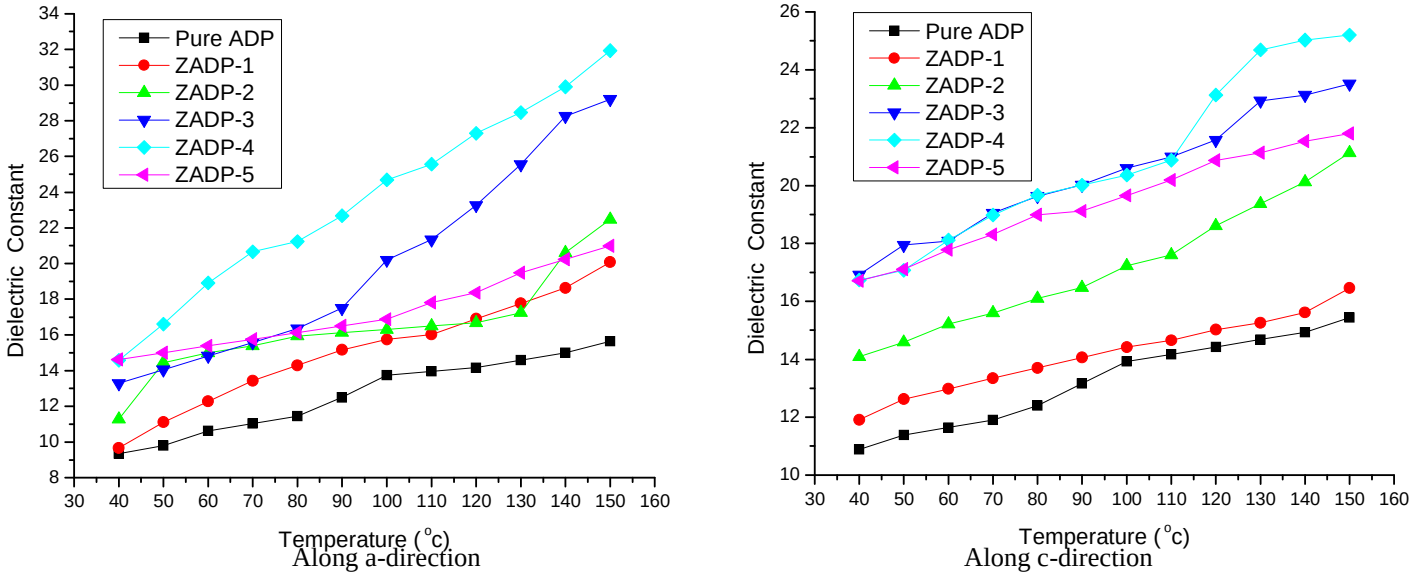

Along a-direction Along c-direction

Fig.8: Dielectric constants (ε_r) observed for the Pure and ZnS doped ADP crystals

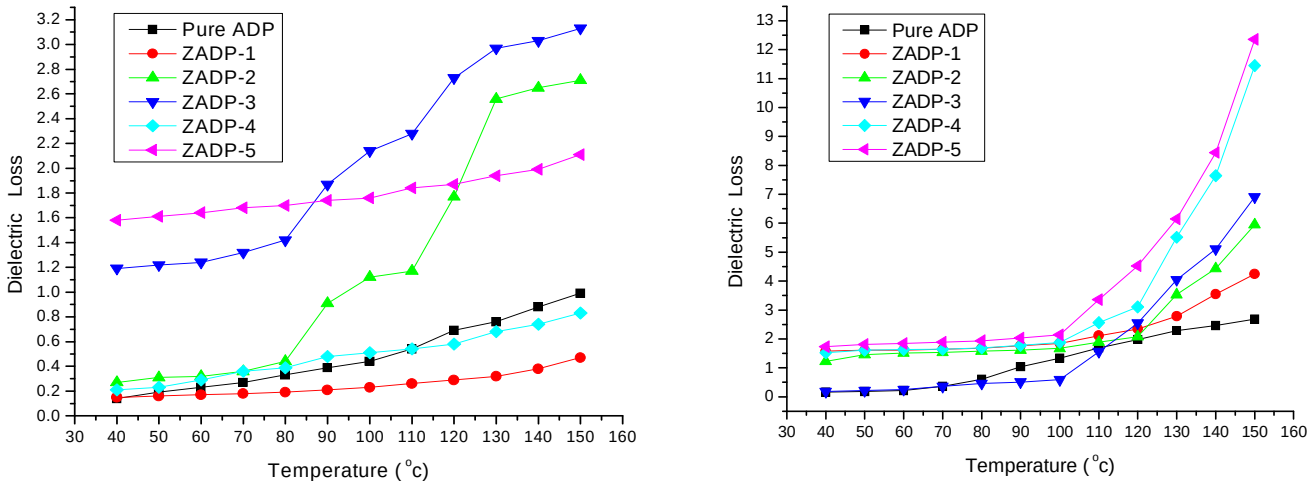

Along a-direction Along c-direction

Fig.9: Dielectric loss factors (tan δ) observed for the Pure and ZnS doped ADP crystals

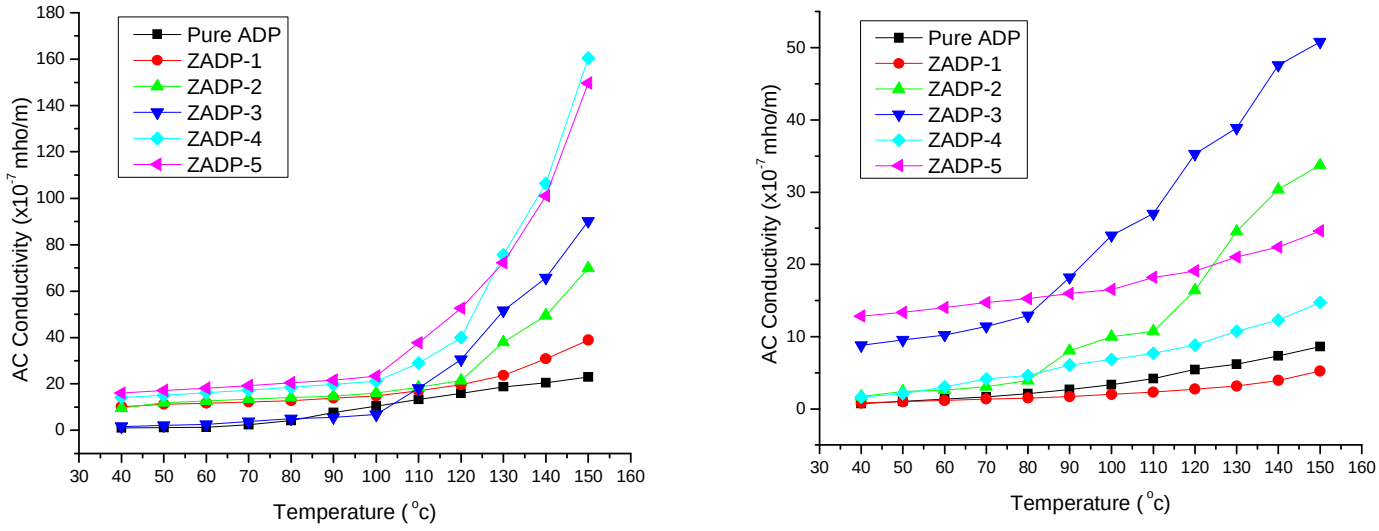

Along a-direction Along c-direction

Fig.10: AC electrical conductivities (σ_{ac}) observed for the Pure and ZnS doped ADP crystals

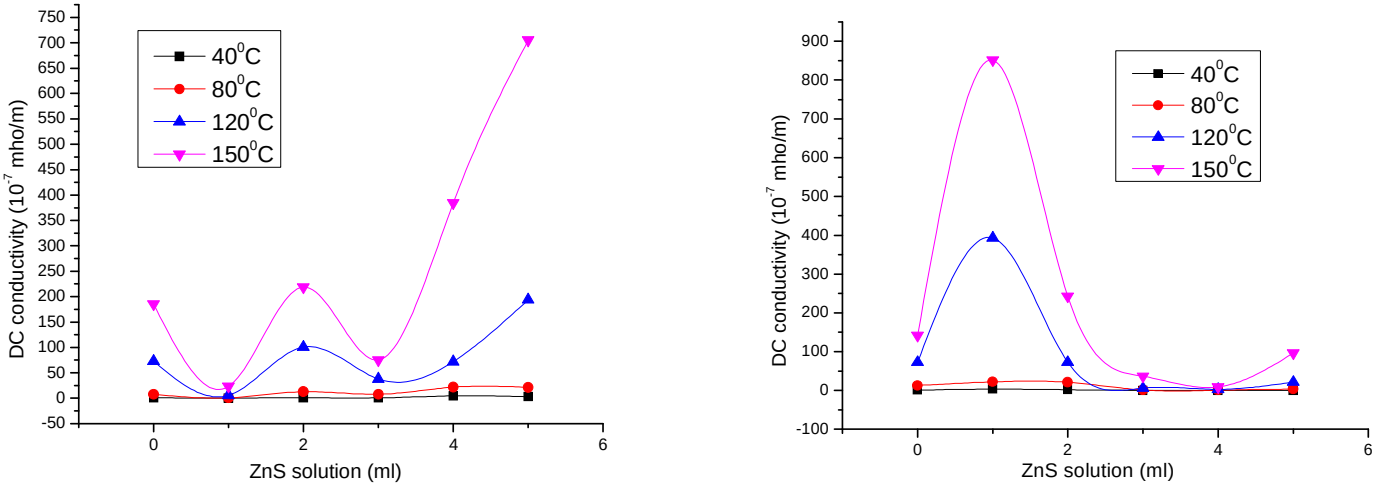

Along a-direction Along c-direction

Fig.11: Impurity concentration dependence of (σ_{dc}) observed for the Pure and ZnS doped ADP crystals

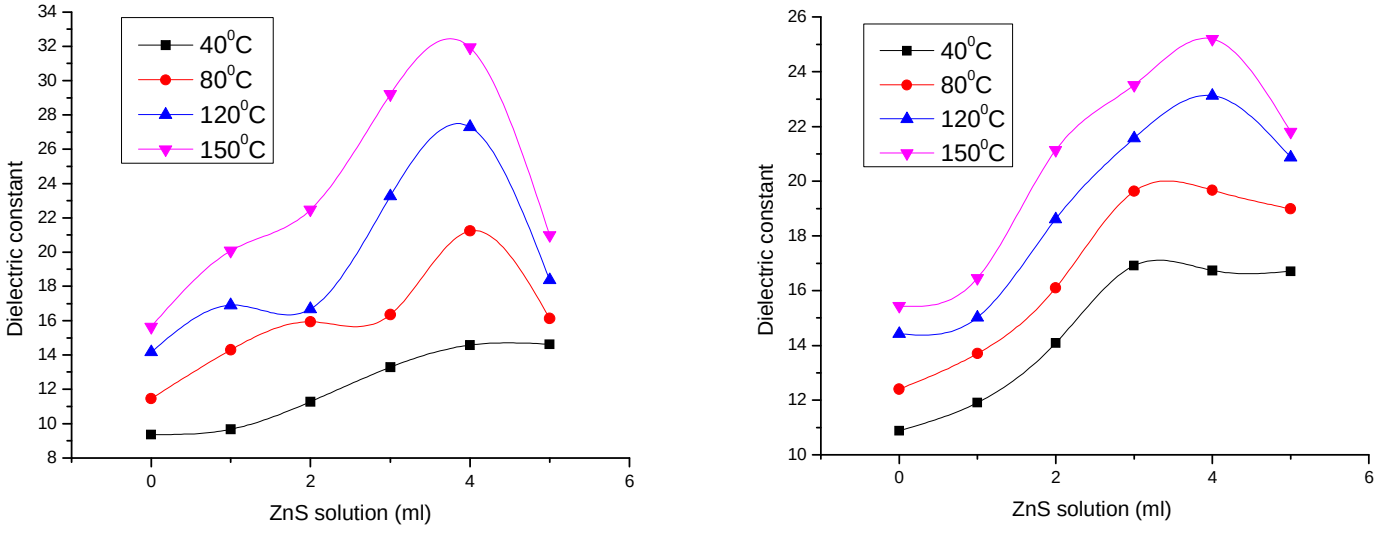

Along a-direction Along c-direction

Fig.12: Impurity concentration dependence of (ε_r) observed for the Pure and ZnS doped ADP crystals

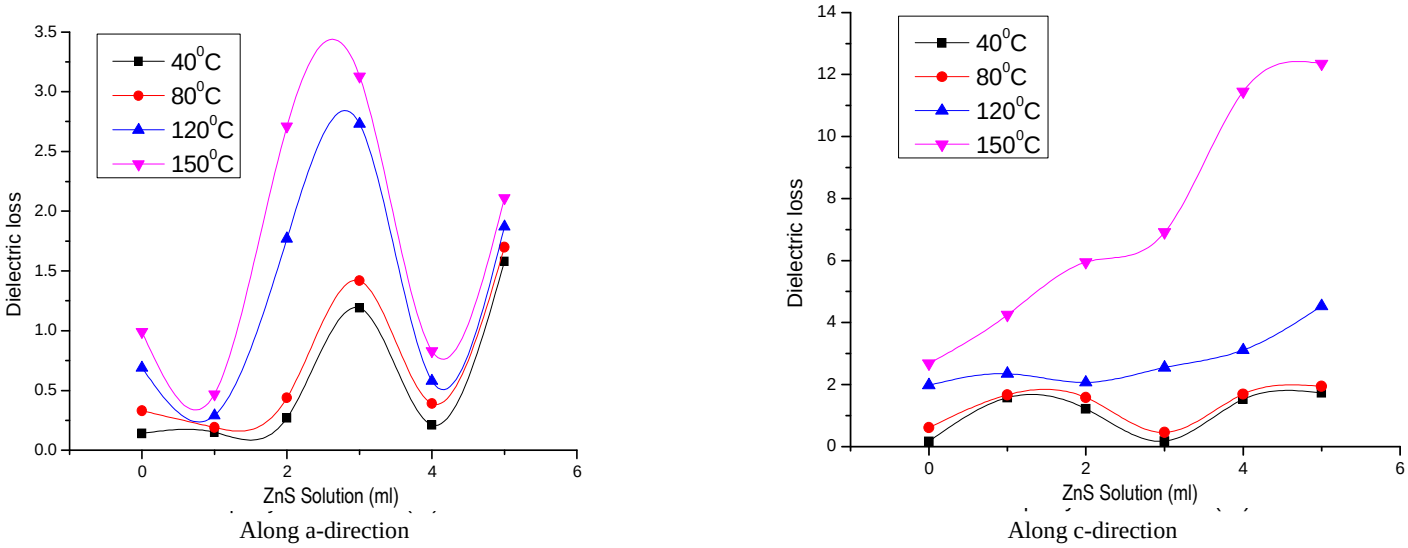

Fig.13: Impurity concentration dependence of ($tan\delta$) observed for the Pure and ZnS doped ADP crystals

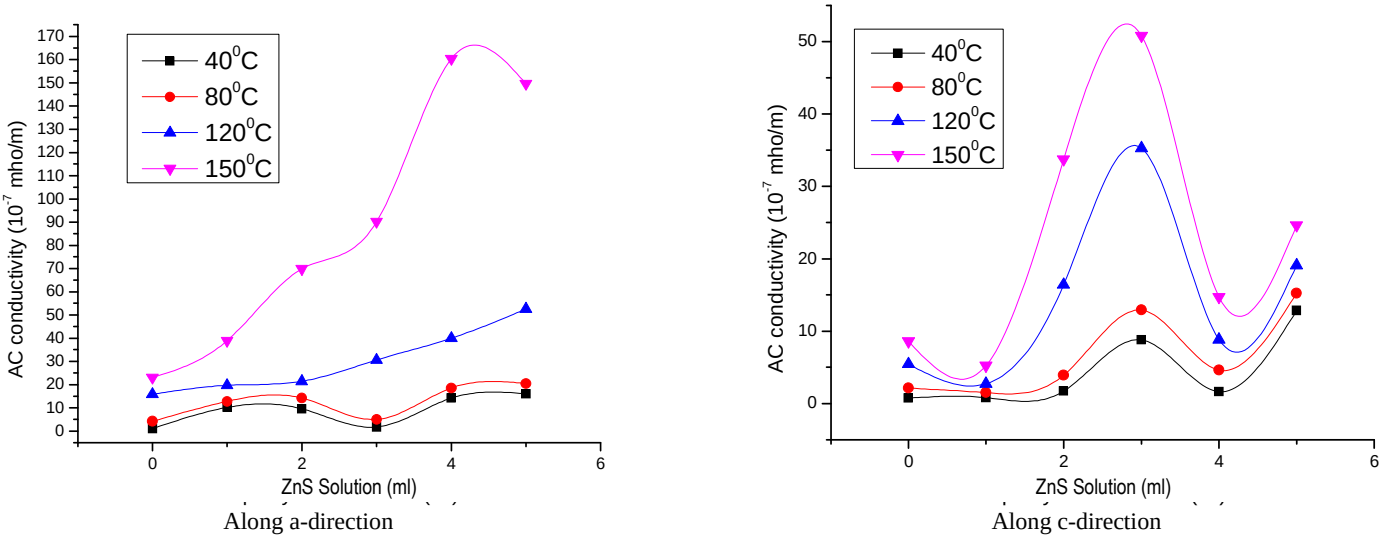

Fig.14: Impurity concentration dependence of (σ_{ac}) observed for the Pure and ZnS doped ADP crystals

Table-4: The activation energies (E_{dc} and E_{ac}) estimated for the pure and ZnS doped ADP crystals

Crystal	Activation energies (eV)			
	Along a - direction		Along c - direction	
	E_{ac}	E_{dc}	E_{ac}	E_{dc}
Pure ADP	0.111	0.275	0.163	0.270
ZADP-1	0.078	0.249	0.052	0.294
ZADP-2	0.144	0.233	0.077	0.292
ZADP-3	0.097	0.277	0.189	0.213
ZADP-4	0.095	0.258	0.106	0.197
ZADP-5	0.028	0.246	0.033	0.248

The increase of conductivity with the increase in temperature observed for Pure and ZnS doped ADP single crystals in the present study is similar to that observed for several other inpurities by previous authors [51]. This can be understood as due to the temperature dependence of the proton transport. Moreover, the conductivity increases smoothly through the temperature range considered in the present study. The estimated activation energies (E_{dc} and E_{ac}) for the pure and ZnS doped ADP crystals grown in the present study are provided in Table 4. E_{ac} values are observed to be less than the E_{dc} values as excepted. The low values of E_{dc} and E_{ac} observed suggest that oxygen vacancies may be responsible for electrical conduction in the temperature region considered.

The temperature variation of dielectric constant is generally attributed to the electronic and ionic polarizations, crystal expansion, the presence of impurities and crystal defects. The increase of ε_r at higher temperatures is mainly attributed to the thermally generated charge carries and impurity

dipoles. The increase of ε_r at lower temperatures is mainly attributed to the crystal expansion and electronic and ionic polarizations. Varotsos [61] has shown that, in the case of ionic crystals, the electronic polarizability practically remains constant. So, it can be understood that the temperature dependence of ε_r observed in the case of pure and ZnS doped ADP crystals is essentially due to the temperature variation of ionic polarizability.

When it dissolves in the solvent, as it is an ionic substance, the ZnS is expected to become Zn^{2+} and S^{2-} ions. So, in the ADP crystal matrix, some of these ions are expected to occupy the interstitial positions and, to some extent, the impurity ions are expected to replace the ions in ADP. This induces bulk defect states due to competition in gething the sites for the impurity ions to occupy and, consequently, it is expected to create a random disturbance in the hydrogen bonding system in the ADP crystal matrix. Hence, as the conduction in ADP crystal is protonic, the random disturbance in the hydrogen bonding system may cause the electrical parameters to vary nonlinearly with the impurity concentration.

CONCLUSIONS

Ethylene diamine capped ZnS nanoparticles were prepared by a simple solvothermal method using a domestic microwave oven. The solubility of ZnS nanoparticles is found to be 0.71g/100 ml of water. So, ZnS doped ADP single crystals could be grown successfully by the free evaporation method at room temperature from aqueous solutions and characterized structurally, chemically, thermally, optically, mechanically and electrically. Results obtained in the present study indicate that the ZnS molecules have entered into the ADP crystal matrix. Also, the ZnS addition has been found to enhance the SHG efficiency significantly and tune the optical and electrical properties.

REFERENCES

[1]. Dongfeng Xue, Siyuan Zhang, *J. Phys. and Chem. Solids*, 57, 1321, 1996

[2]. N.P.Rajesh, K.Meera, K.Srinivasan, P.Santhana Raghavan, P.Ramasamy, *J. Cryst. Growth*, 213, 389, 2000

[3]. A.P.Bhat, P.S.Aithal, P.Mohan Roa, D.K.Avasthi, *Nuclear Insturments and Methods in Physics Research B*, 964, 166, 2000

[4]. Dongli Xu, Dongfeng Xue, *J. Cryst. Growth*, 242, 144, 2006

[5]. V.Tripadus, M.Gugiu, M.Statescu, A.Podlesnyak, *Chemical Phys.*, 335, 233, 2007.

[6]. Dongli Xu, Dongfeng Xue, *J. Cryst. Growth*, 310, 1385, 2008

[7]. L.Tenzer, B.C.Frazer, R.Pepinsky, *Acta Cryst.*, 11, 505, 1958

[8]. M.E.Lines, A.M.Glass, *Principles and Applications of Ferroelectrics and Related Materials*, Clarendon Press, Oxford, 1977

[9]. N.G.Parsonage, L.A.K.Staveley, *Disorder in Crystals*, Clarendon Press, 1978

[10]. J.W.Mullin, A.Amatavivadhana, *J. App. Chem.*, 17, 151, 1967

[11]. N.P.Rajesh, V.Kannan, P.Santhana Raghavan, P.Ramaswamy and C.W.Lan, *Materials Chem. and Phys.*, 76, 181, 2002

[12]. A.Anne Assencia and C.Mahadevan, *Bull of Mater. Sci.*, 28, 415, 2005

[13]. A.Jayarama, S.M.Dharmaprakash, *Indian J.Pure App. Phy.*, 43, 859, 2005

[14]. A.Claudc, V.Vaithianathan, R.Bairava Ganesh, R.Sathya Lakshmi, P.Ramasamy, *J. App. Sci.*, 6 (1) 85, 2006

[15]. D.L.Xu and D.F.Xue, *J. Crys. Growth*, 286, 108, 2006

[16]. P.V.Dhanaraj, G.Bhagavanarayana and N.P.Rajesh, *Mat. Chem. Phys.*, 112, 490, 2008

[17]. P.Rajesh, P.Ramasamy, C.K.Mahadevan, *J.Cryst. Growth*, 311, 1156, 2009

[18]. P.Rajesh and P.Ramaswamy, *Mater. Lett.*, 63, 2260, 2009

[19]. P.Rajesh, P.Ramasamy, G.Bhagavanarayana, *J.Cryst. Growth*, 311, 4069, 2009

[20]. G.G.Muley, M.N.Rode, S.A.Waghuley, B.H.Pawar *Opto Electronics and Advan. Mater*, 4, 11, 2010

[21]. Ferdousi Akhtar and Jiban Podder, *J. Cryst. Process and Tech.*, 1, 18, 2011

[22]. P.Rajesh, K.Boopathi, P.Ramasamy, *J. Cryst. Growth*, 318, 751, 2011

[23]. I.Pritula, V.Gagvoronskg, M.Kopylovskg, M.Kolybaeva, V.Puzikov, A.Kosinova, V.T.Kachenko, V.Tsurikov, T.Konstantiniva, V.Pogibko, *Functional Mater.*, 15, 420, 2008

[24]. V.Ya.Gayvoronsky, V.N.Starkov, M.A.Kopylovsky, M.S.Brodyn, E.A.Vishnyakov, A.YU.Boyarchuk, I.M.Pritula, *Ukr. J.Phys.* 55, 875, 2010

[25]. I.Pritula, O.Bezkrovnaya, M.Kolybayeva, A.Kosinova, D.Sofronov, V.Tkachenko, V.Tsurikov, *Mater. Chem. and Phys.*, 129, 777, 2011

[26]. V.Ya.Gayvoronsky, M.A.Kopylovsky, V.O.Yatsyna, A.S.Popov, A.V.Kosinova, I.M.Pritula, *Functional Mater.*, 19, 54, 2012

[27]. V.Ya.Gayvoronsky, M.A.Kopylovsky, V.O.Yatsyna, A.I.Rostotsky, M.S.Brodyn, I.M.Pritula, *Ukr.J.Phys.*, 57, 159, 2012

[28]. Valentin G.Grachev, Ian.A.Vrable, Galina, I.Malovichko, Igor M.Pritula, Olga N.Bezkrovnaya et al., *J.Appl.Phys.* 112, 014315(1-10), 2012

[29]. V.Ya.Gayvoronsky, M.A.Kopylovsky, M.S.Brodyn, I.M.Pritula, M.I.Kolybaeva, V.M.Puzikov, *Laser Phys. Lett.*10, 035401 (1-5), 2013

[30]. A.Bensouici, J.L.Plaza, O.Halimi, B.Boudine, M.Sebais, E.Dieguez, *J.Optoelectronics and Adv.Materials*, 10, 3051, 2008

[31]. I.Pritula, V.Gayvonsky, YU.Gromov, M.Kopylosky, M.Kolybaeva, V.Puzikov, A.Kosinova, Yu.Savvin, Yu.Velikhov, A.Levchenko, *Optics Communications*, 282, 1141, 2009

[32]. M.Abdulkhadar, B.Thomas, *Nanostruct. Mater.*, 5 (3), 289, 1995

[33]. V.Albe, C.Jouanin, D.Bertho, *J.Cryst. Growth*, 184/185, 388, 1998

[34]. L.Saviot, B.Champagnon, E.Duval, A.I.Ekimov, *J.Cryst. Growth*, 184/185, 370 1998
[35]. B.Boudine, M.Sebais, O.Halimie, H.Alliouche, A.Boudrioua, R.Mouras, *Catalysis Today*, 89, 293, 2004
[36]. B.Boudine, M.Sebais, O.Halimi, R.Mouras, A.Boudrioua, P.Bourson, *Optical Mater.*, 25, 373, 2004
[37]. A.Bensouici, J.L.Plaza, E.Dieguez, O.Halimi, B.Boudine, S.Addala, L.Guerbous, M.Sebais, *J.Luminescence*, 129, 948, 2009
[38]. K.Balasubhramanian, P.Selvarajan, E.Kumar, *Indian Journal of Science and Technology*, 3 (1), 41, 2010
[39]. X.D.Gao, X.M.Li, W.D.Yu, *Thin Solid Films*, 468, 43, 2004
[40]. S.H.Deulkara, C.H.Bhosale, M.Sharonb. *J.Phys. Chem. Solids*, 65, 1879, 2004
[41]. J.Vidal, O.DeMelo, O.Vigil, N.Lopez, G.Contreras-Puente, O.Zelaya-Angel, *Thin Solid Films*, 419, 118, 2002
[42]. Y.Andrew wang, J.Jack Li, Haiyan Chen, Xiaogang Peng, *J.Am.Chem. Soc.*, 124, 2293, 2002
[43]. Wenzhou Guo, J.Jack Li, Y.Andrew Wang, Xiaogang peng. *Chem. Mater.*, 15, 3125, 2003
[44]. Tang, Mi Yan, Hui zhang, Minzhe xia, Daren Yang, *Mater. Lett.*, 59, 1024, 2009
[45]. R.S.S.Saravanan, C.K.Mahadevan, J.*Alloys and Compounds*, 541, 115, 2012
[46]. S.I.Srikrishna Ramya, C.K.Mahadevan, *Mater.Lett.*, 89, 111, 2012
[47]. S.Nagaveena, C.K.Mahadevan *J.Alloys and Compounds*, 582, 447, 2013
[48]. H.Lipson and H.Steeple *Interpretation of X-ray powder diffraction patterns*, MacMilan, Newyork, 1970
[49]. S.K.Kurtz, T.T.Perry, *J.Appl. Phys.* 39, 3798, 1968
[50]. T.H. Freeda, C. Mahadevan *Bull. Mater.Sci.*, 23, 335, 2000
[51]. M.Meena, C.K.Mahadevan, *Cryst.Res. Technol.*, 43. 166, 2008
[52]. M.Priya, C.K. Mahadevan *Physica B*, 403, 67, 2008
[53]. C.K. Mahadevan and K. Jayakumari, *Physica B*, 403, 3990, 2008
[54]. S.Goma, C.M. Padma, C.K.Mahadevan, *Mater.Lett.*, 60,3701,2006
[55]. M.Meena, C.K.Mahadevan, *Mater. Lett.*, 62, 3742, 2008
[56]. S.Chaki, M.P.Deshpande, J.P.Tailor, M.D.Chaudhary, K.Mahato, *Am. J. Condensed Matter Phys.*, 2 (1), 22, 2012
[57]. P.V.Dhanaraj, N.P.Rajesh, *Crystallisation and material Science of Modern artificial and natural crystals* (Edited by Dr.Elena Borisenko Pp.79, 2012)
[58]. S.Karan, S.P.Sen Gupta, *Mater. Sci. Eng.*, A398, 198, 2005
[59]. M.V.Artemyev, V.Sperling, U.Woggon, *J. Appl. Phys.*, 81 (10), 6975, 1997
[60]. P.Rajesh and P.Ramaswamy, *Physica B*, 404, 1611, 2009
[61]. P.Varotsos, *J.Phys. Lett.*, 39, L79, 1978

BIOGRAPHIES

Anitha Hudson born in Nagercoil, India in 1976, has acquired her academic degrees B.Sc. (Physics, 1996), M.Sc. (Physics, 1998) from Madurai Kamaraj University and M.Phil. (Physics, 2000) from Manonmaniam Sundaranar University. She is a Ph.D. research Scholar of Manonmaniam Sundaranar University. She has about 3 years research experience in the field of Crystal growth and characterization.

C.K.Mahadevan, born in Nagercoil, India in 1958 has acquired B.Sc.(1978), M.Sc.(1980), Ph.D.(1984) and D.Sc. (2002) degrees in Physics from reputed institutions in India. After serving for some time in different places in India and USA, he started his long service in S.T.Hindu College, Nagercoil in 1987 and has been there till Date. He has more than 27 years teaching experience (taught B.Sc., M.Sc., M.Phil and Ph.D. students) and 32 years research experience (guided 30 Ph.D. projects, published 1 review article and 180 research papers in International journals and delivered 57 invited talks in national/international conferences). His major research area is Crystalline and Nanostructured Materials Science (Materials Synthesis and Characterization). He is a winner of several coveted awards and honours for his teaching, research and related activities.

C.M.Padma born in Marthandam, India in 1962, had acquired her academic degrees B.Sc. (Physics, 1982) and M.Sc. (physics, 1984) from Madurai Kamaraj University and M.Phil. (Physics, 2000) and Ph.D (Physics, 2008) from Manonmaniam Sundaranar University. She has about 28 years teaching experience (taught B.Sc., M.Sc., M.Phil., and Ph.D. students) in Women's Christian College, Nagercoil. Currently she is an associate professor and head of the department of Physics. She has about 11 years research experience and published more than 10 research papers in International journals and several more papers in conference proceedings. Presently she is guiding 8 Ph.D. projects and her research area is crystal growth and characterization.